Tensor decomposition exploiting structural constraints for brain source imaging

Ahmad Karfoul

joint work with

Hanna Becker, Laurent Albera,
Rémi Gribonval, Julien Fleureau, Philippe Guillotel,
Amar Kachenoura, Lotfi Senhadji, Isabelle Merlet

One-Day workshop on tensors and covariance matrix estimation

November 2015 - Marseille

1. Motivation

EEG and MEG:
Multisensor systems that record brain activity with a high temporal resolution

www.canada-meg-consortium.org

- Objective: Separation and localization of brain sources
- Applications:
  - Diagnosis and management of diseases such as epilepsy
    $\Rightarrow$ e.g., identification of epileptogenic zones
  - Neuroscience: Understanding of brain functions

1. Motivation

❒ **Tensor-based approaches for EEG source separation:**

Exploited dimensions in addition to space and time:

- frequency [1]
- wave vector [2]
- subject [3]
- realization [4]

Employed tensor model:

- Canonical Polyadic (CP) decomposition [1,2]
- PARAFAC2 [5]
- Shift-invariant CP (SCP) [6]
- Block term decomposition [7]

[1] Miwakeichi et al. 2004
[2] Becker et al. 2012
[3] Morup et al. 2006
[4] Deburchgraeve et al. 2009
[5] Weis et al. 2010
[6] Morup et al. 2008
[7] Hunyadi et al. 2014

1. Motivation

- Tensor-based approaches for EEG source separation:

Exploited dimensions in addition to space and time:
- frequency [1]
- wave vector [2]
- subject [3]
- realization [4]

Employed tensor model:
- Canonical Polyadic (CP) decomposition [1,2]
- PARAFAC2 [5]
- Shift-invariant CP (SCP) [6]
- Block term decomposition [7]

$\Rightarrow$ Tensor decomposition results are mostly used to identify spatial maps and time signals of the sources

- Idea: improve interpretation of EEG by identifying the source positions and their spatial extents ➔ brain source imaging

Outline

1. Motivation

2. Data Model

3. CP Tensor decomposition

4. Tensor - based source localization
   - Classical two-steps approach
   - Proposed single - step approach

5. Simulations

6. Conclusion

2. Data model

$$\boxed{\mathbf{X} = \mathbf{G} \cdot \mathbf{S} \in \mathbb{R}^{N \times T}}$$

$$\mathbf{G} \in \mathbb{R}^{N \times D}$$

- Lead field matrix: depends on spatial parameters

$\boxed{N \text{ - number of sensors}}$

$$\mathbf{S} \in \mathbb{R}^{D \times T}$$

- Signal matrix: temporal behavior of *D* dipoles

$\boxed{T \text{ - number of time samples}}$

2. Data model

- EEG data matrix: $$\boxed{\mathbf{X} = \mathbf{G} \cdot \mathbf{S} \in \mathbb{R}^{N \times T}}$$

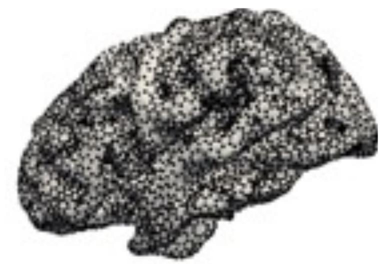

$$\mathbf{G} \in \mathbb{R}^{N \times D} \qquad \mathbf{S} \in \mathbb{R}^{D \times T}$$

  - Lead field matrix: depends on spatial parameters
    $\boxed{N \text{ - number of sensors}}$
  - Signal matrix: temporal behavior of *D* dipoles
    $\boxed{T \text{ - number of time samples}}$

- Distributed source model:

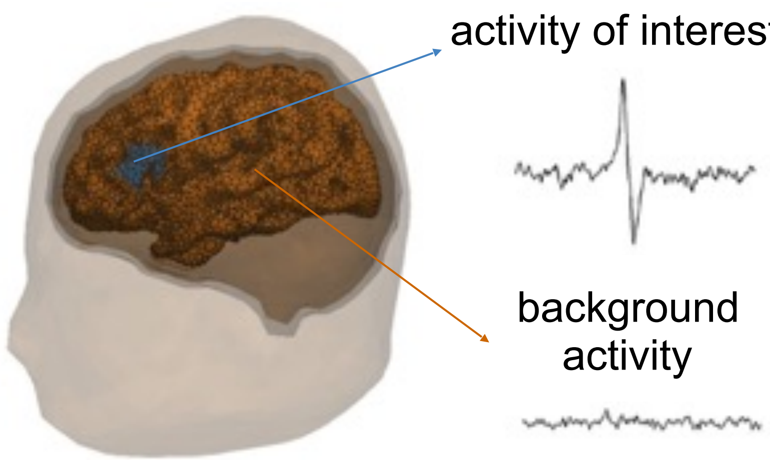

$$\Rightarrow \mathbf{X}_e$$

$$\Rightarrow \mathbf{X}_b$$

2.1 Example of a patch

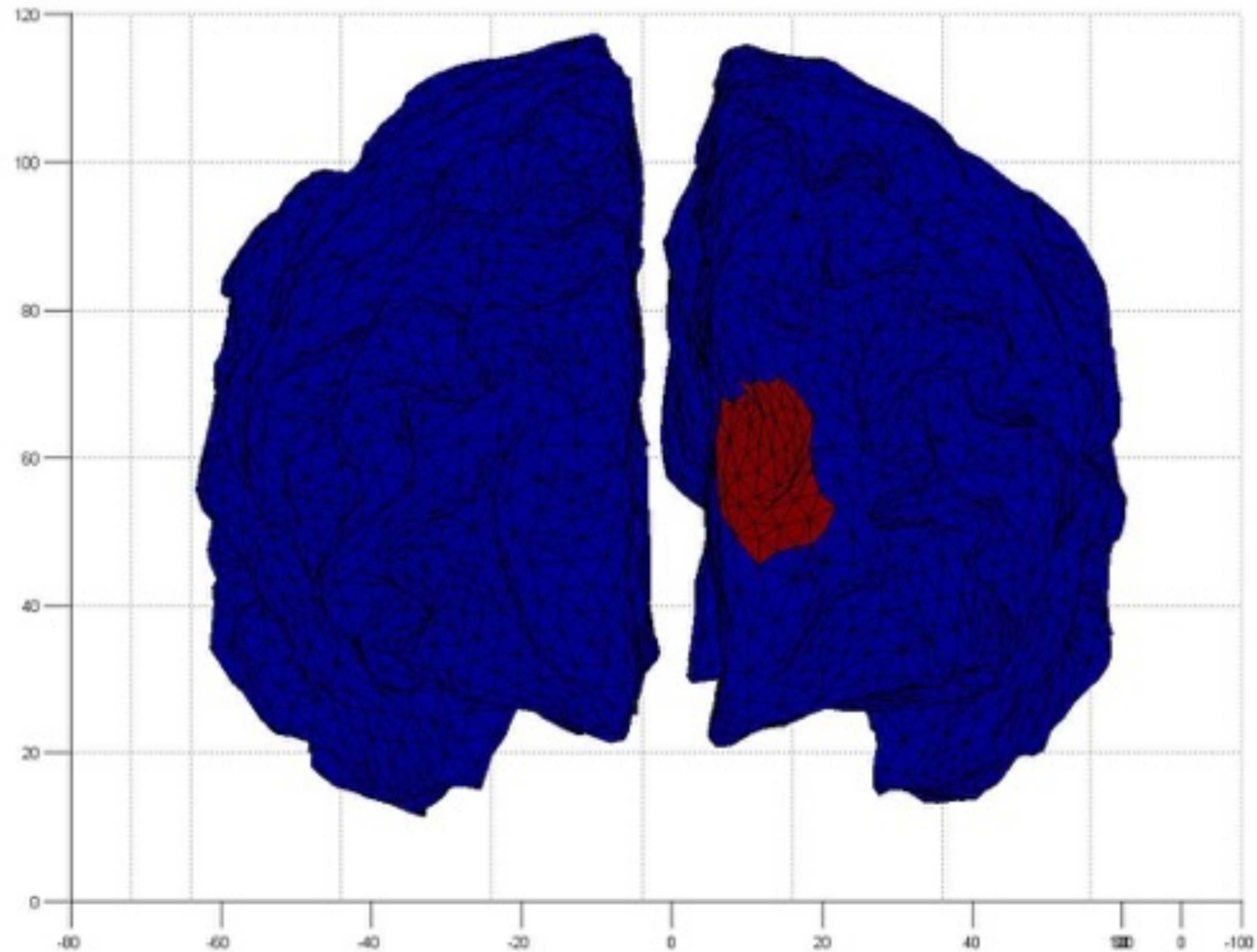

2. Data model

- EEG data matrix: $\boxed{\mathbf{X} = \mathbf{G} \cdot \mathbf{S} \in \mathbb{R}^{N \times T}}$

$$\mathbf{G} \in \mathbb{R}^{N \times D} \qquad \mathbf{S} \in \mathbb{R}^{D \times T}$$

  - Lead field matrix: depends on spatial parameters
    $\boxed{N \text{ - number of sensors}}$
  - Signal matrix: temporal behavior of *D* dipoles
    $\boxed{T \text{ - number of time samples}}$

- Distributed source model:

$$\mathbf{X} = \mathbf{X}_e + \mathbf{X}_b = \sum_{p=1}^{P} \mathbf{h}_p \mathbf{s}_p^{\mathrm{T}} + \mathbf{X}_b$$

$\boxed{P \text{ - number of sources}}$

$\mathbf{h}_p = \mathbf{G}\psi_p$ distributed source lead field vector

ψ_p – coefficient vector

average signal of the p-th source

3. CP tensor decomposition

- Essentially unique (up to scale and permutation indeterminacies) under mild conditions
- Approximates a tensor by P rank-1 components:

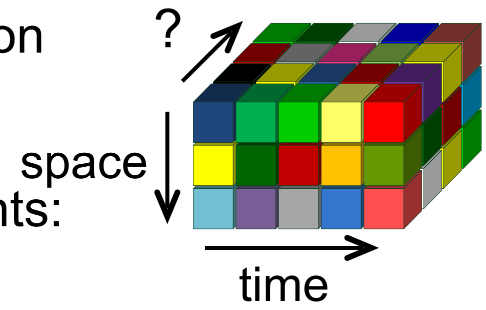

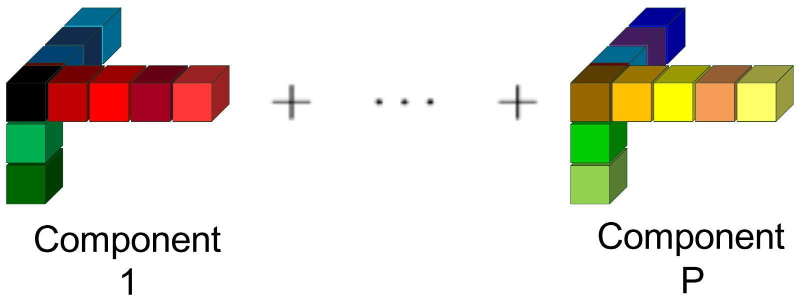

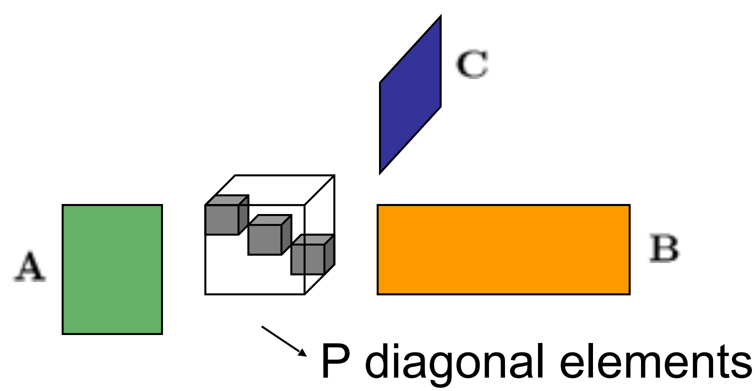

3. CP tensor decomposition

- Essentially unique (up to scale and permutation indeterminacies) under mild conditions
- Approximates a tensor by P rank-1 components:

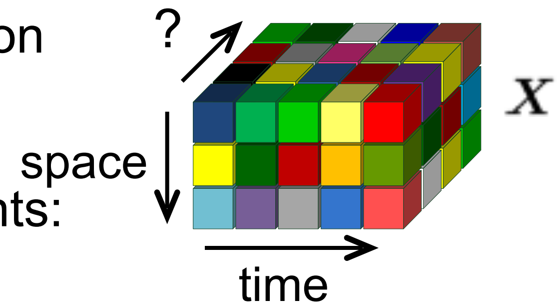

$$\boldsymbol{X} \approx \sum_{p=1}^{P} \mathbf{a}(p) \circ \mathbf{b}(p) \circ \mathbf{c}(p)$$

$$\boldsymbol{X} \approx \boldsymbol{I} \times_1 \mathbf{A} \times_2 \mathbf{B} \times_3 \mathbf{C}$$

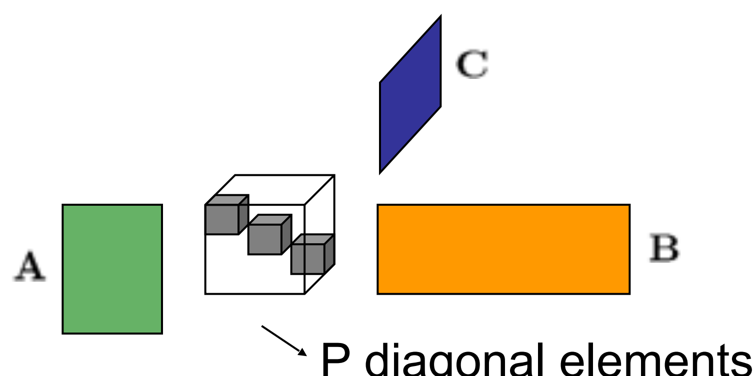

3.1 Space-Time-Frequency (STF) analysis

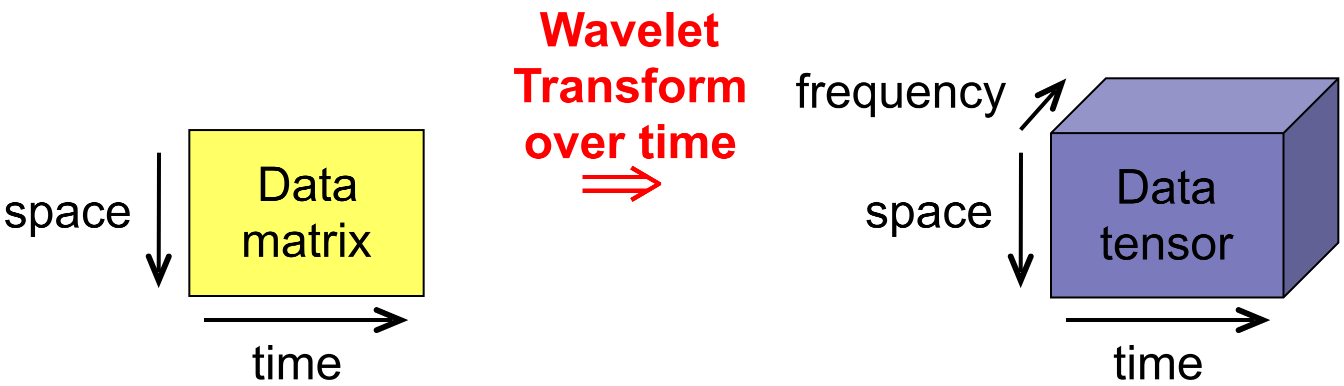

$$W(\mathbf{r}, t, f) = \int_{-\infty}^{\infty} x(\mathbf{r}, \tau) \cdot \psi(a, \tau, t) \mathrm{d}\tau$$

Electric potential data

Wavelet

Exploits temporal changes of the data

3.1 Space-Time-Frequency (STF) analysis

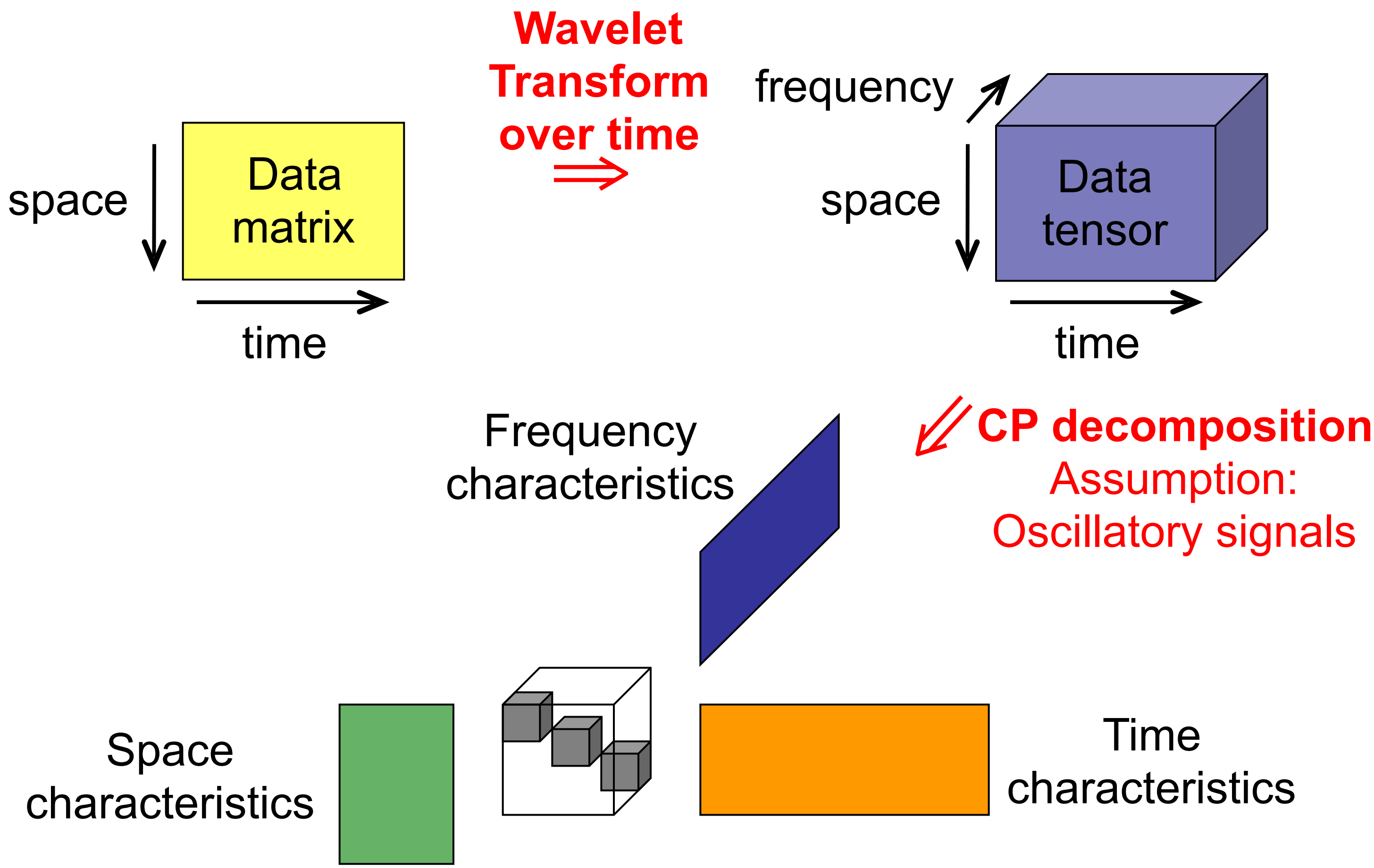

3.1 Space-Time-Frequency (STF) analysis

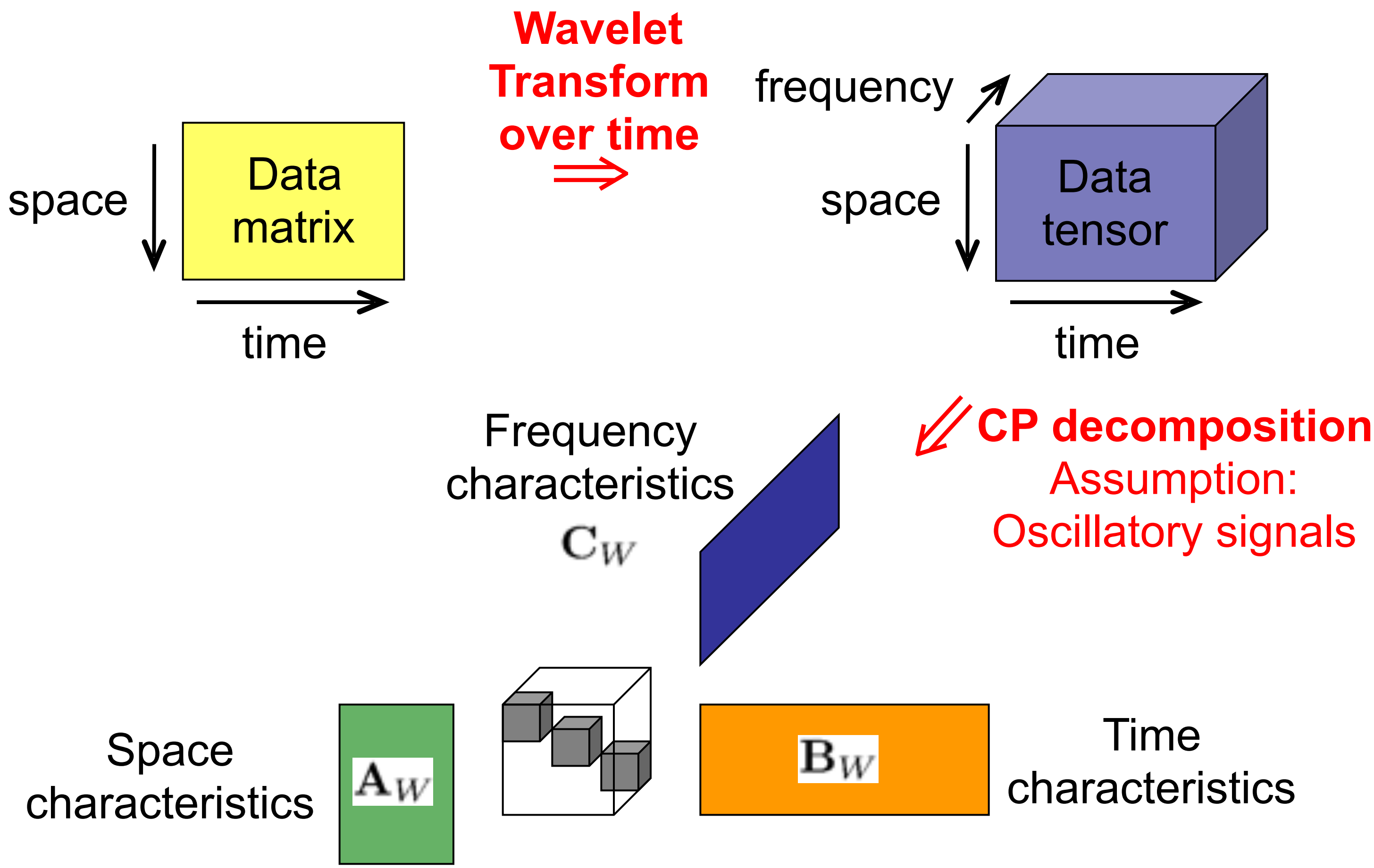

$$W(\mathbf{r},t,f) \approx \sum_{p=1}^{R} \mathbf{a}_W(\mathbf{r};p)\cdot \mathbf{b}_W(t;p)\cdot \mathbf{c}_W(f;p)$$

3.2 Space-Time-Wave-Vector (STWV) analysis

Evaluates spatial changes of the data within a spherical window

3.2 Space-Time-Wave-Vector (STWV) analysis

$$F(\mathbf{r}, t, \mathbf{k}) = \int_{-\infty}^{\infty} w(\boldsymbol{r}' - \boldsymbol{r}) \cdot x(\mathbf{r}', t) e^{j\mathbf{k}^{\mathrm{T}}\mathbf{r}'} \mathrm{d}\mathbf{r}'$$

3D window function

Electric potential data

Evaluates spatial changes of the data within a spherical window

3.2 Space-Time-Wave-Vector (STWV) analysis

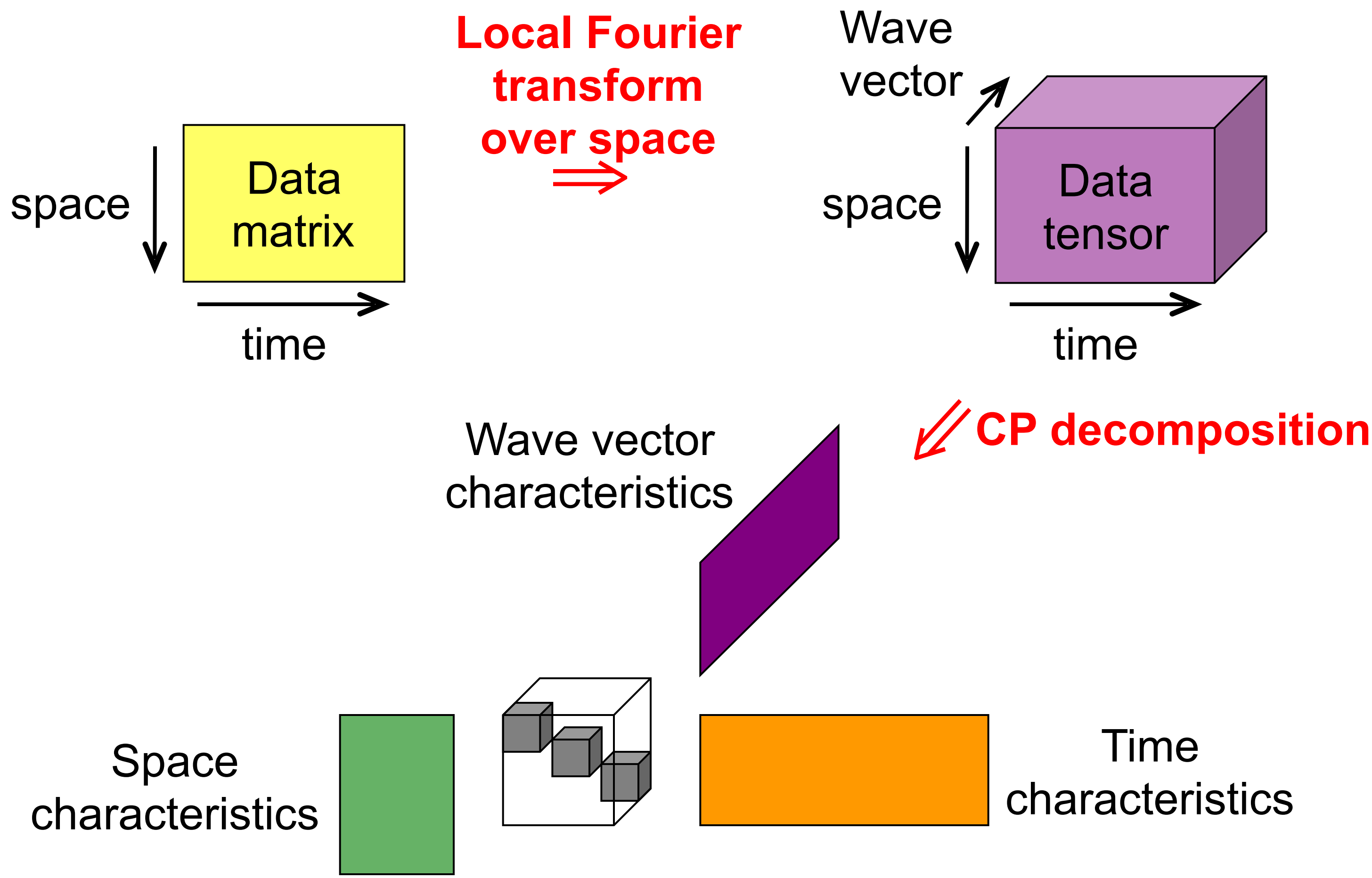

3.2 Space-Time-Wave-Vector (STWV) analysis

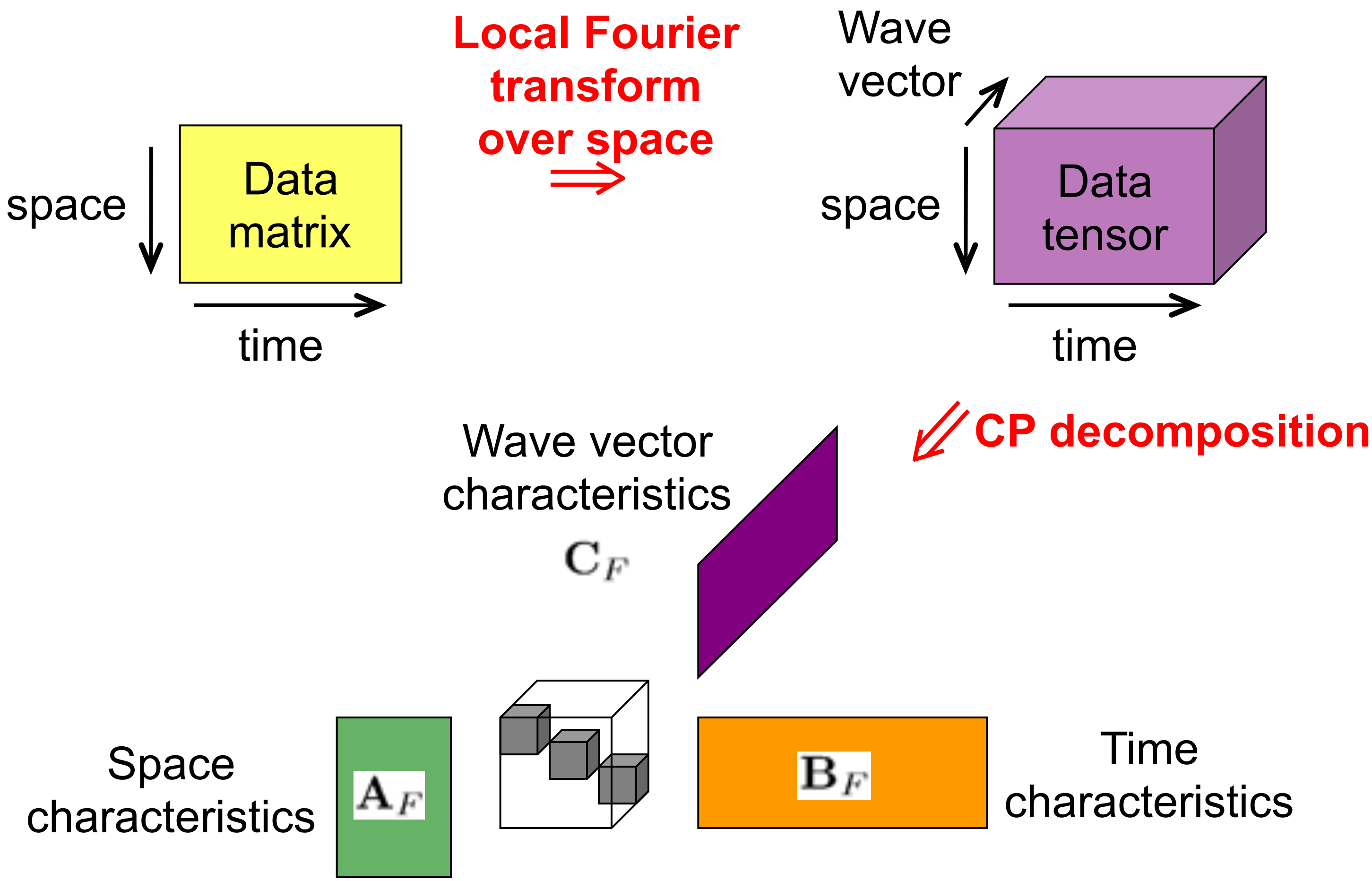

$$\boxed{F(\mathbf{r}, t, \mathbf{k}) \approx \sum_{p=1}^{R} \mathbf{a}_F(\mathbf{r}; p) \cdot \mathbf{b}_F(t; p) \cdot \mathbf{c}_F(\mathbf{k}; p)}$$

3.3 Construction of a space-time-spike tensor

- **Stack EEG data of interictal epileptic spike-like signals observed at different time instants along the third dimension of the tensor [4]**

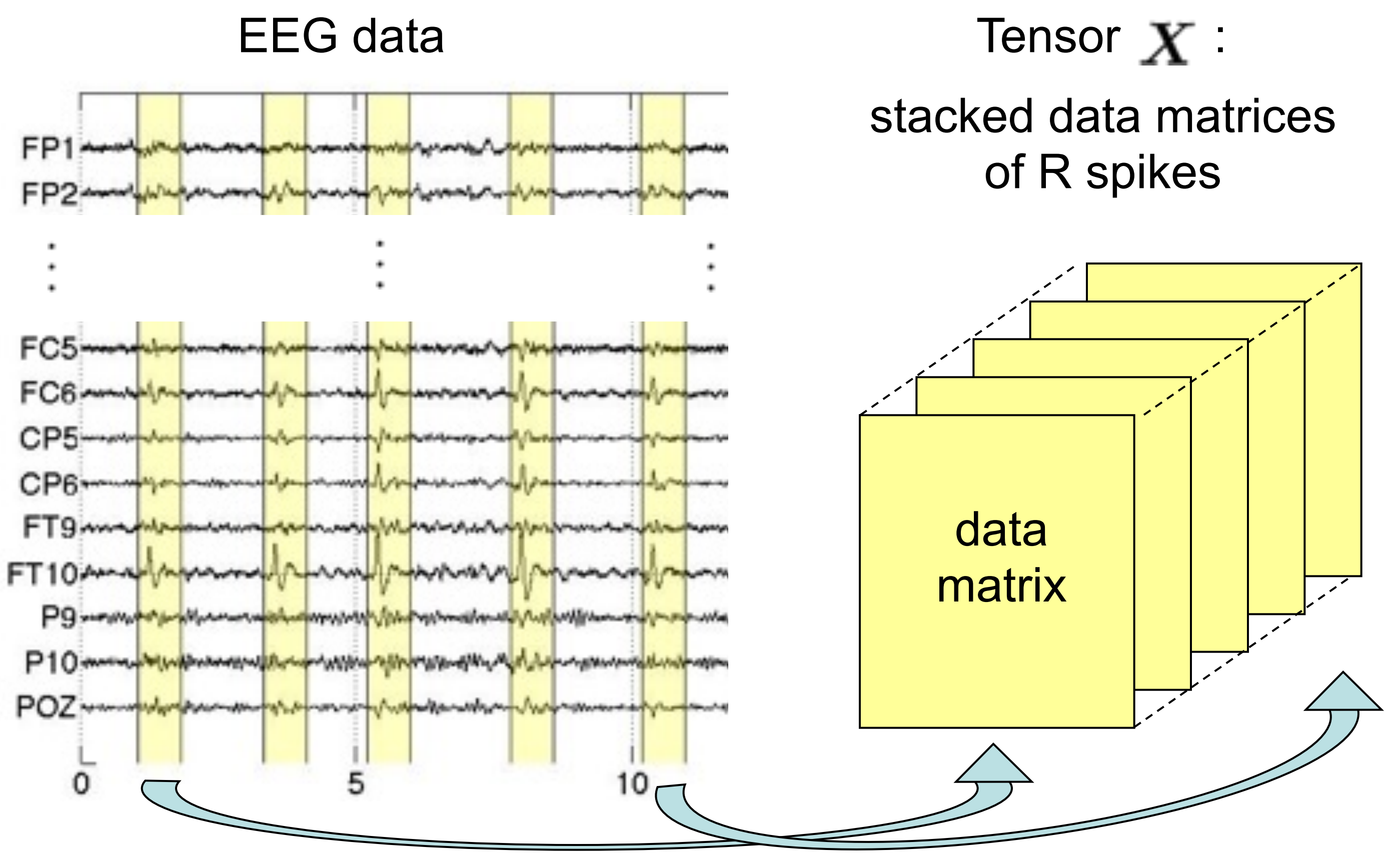

[4] Deburchgraeve et al. 2009 , “Neonatal seizure localization using Parafac decomposition,” Clinical Neurophysiology

3.3 CP model of a space-time-spike tensor

- **CP model:**

$$X \approx \sum_{p=1}^{P} \mathbf{h}_p \circ \mathbf{s}_p \circ \mathbf{c}_p$$

spatial maps | time signals | spike amplitudes

$\mathbf{H} = [\mathbf{h}_1, \ldots, \mathbf{h}_P]$ $\quad \mathbf{S} = [\mathbf{s}_1, \ldots, \mathbf{s}_P]$ $\quad \mathbf{C} = [\mathbf{c}_1, \ldots, \mathbf{c}_P]$

e.g.

p=1

p=2

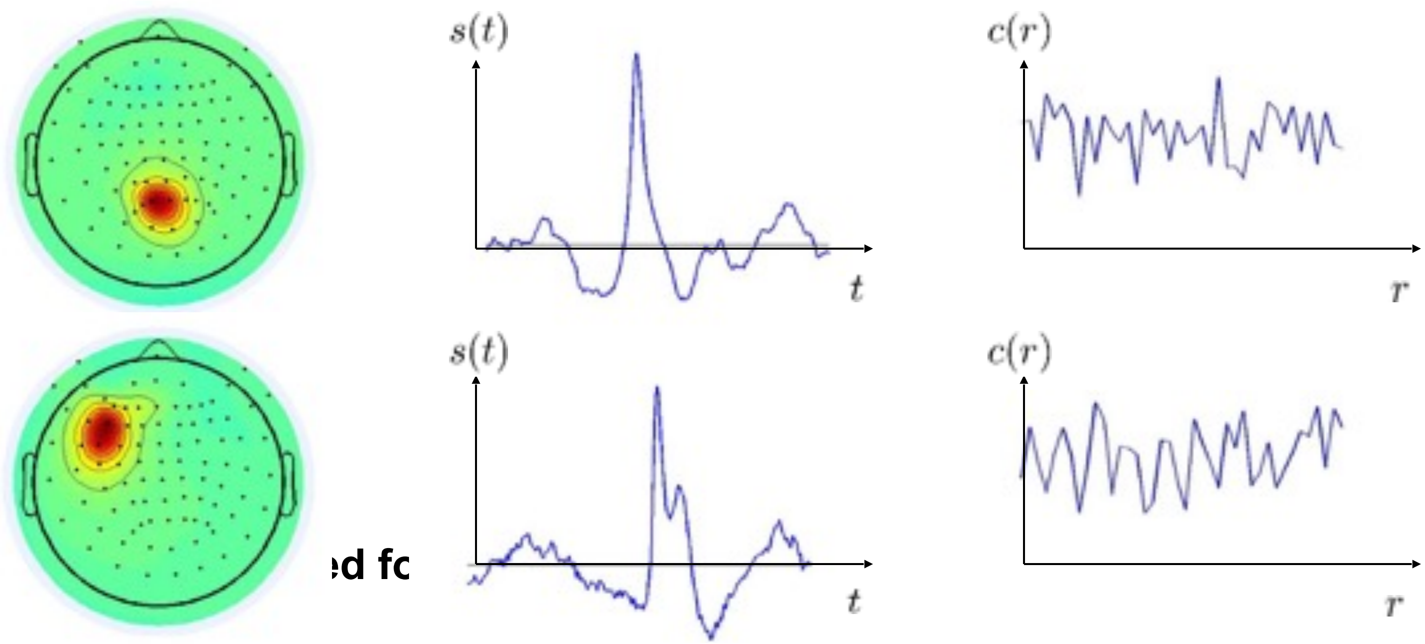

$\Rightarrow$ **spatial** **ed fc**

4.1 Classical two-step tensor-based source localization approach: STS-DA

- **First step: CP decomposition of tensor X to identify the matrix H**

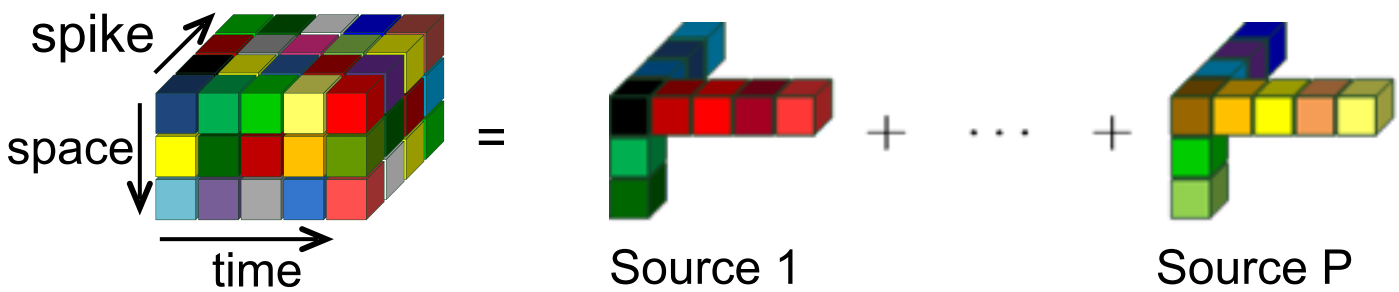

- **Second step: Separate localization of each distributed source based on**
  - **the distributed source lead field vector**
  - **a dictionary of circular-shaped source regions, the "disks". of varying sizes, which are described by the coefficient vectors** $\mathbf{h}_p = \mathbf{G}\psi_p$
  - **a metric**

$$M(\mathbf{h}_p, \psi)$$

4.1 Classical two-step tensor-based source localization approach: STS-DA

- **First step:** **CP decomposition of tensor X to identify the matrix H**

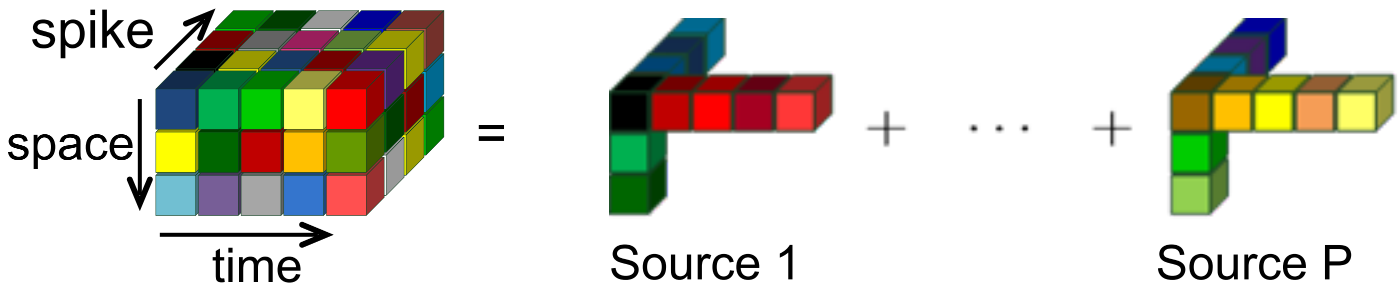

- **Second step:** **Separate localization of each distributed source based on**
  - **the distributed source lead field vector**
  - **a dictionary of circular-shaped source regions, the "disks". of varying sizes, which are described by the coefficient vectors** $\mathbf{h}_p = \mathbf{G}\psi_p$
  - **a metric**

$$M(\mathbf{h}_p, \psi) = \frac{(\hat{\mathbf{h}}_p{}^{\mathsf{T}} \mathbf{G} \boldsymbol{\psi}_p)^2}{\boldsymbol{\psi}_p{}^{\mathsf{T}} \mathbf{G}^{\mathsf{T}} \mathbf{G} \boldsymbol{\psi}_p}$$

4.2 Distributed source localization results: Disk algorithm

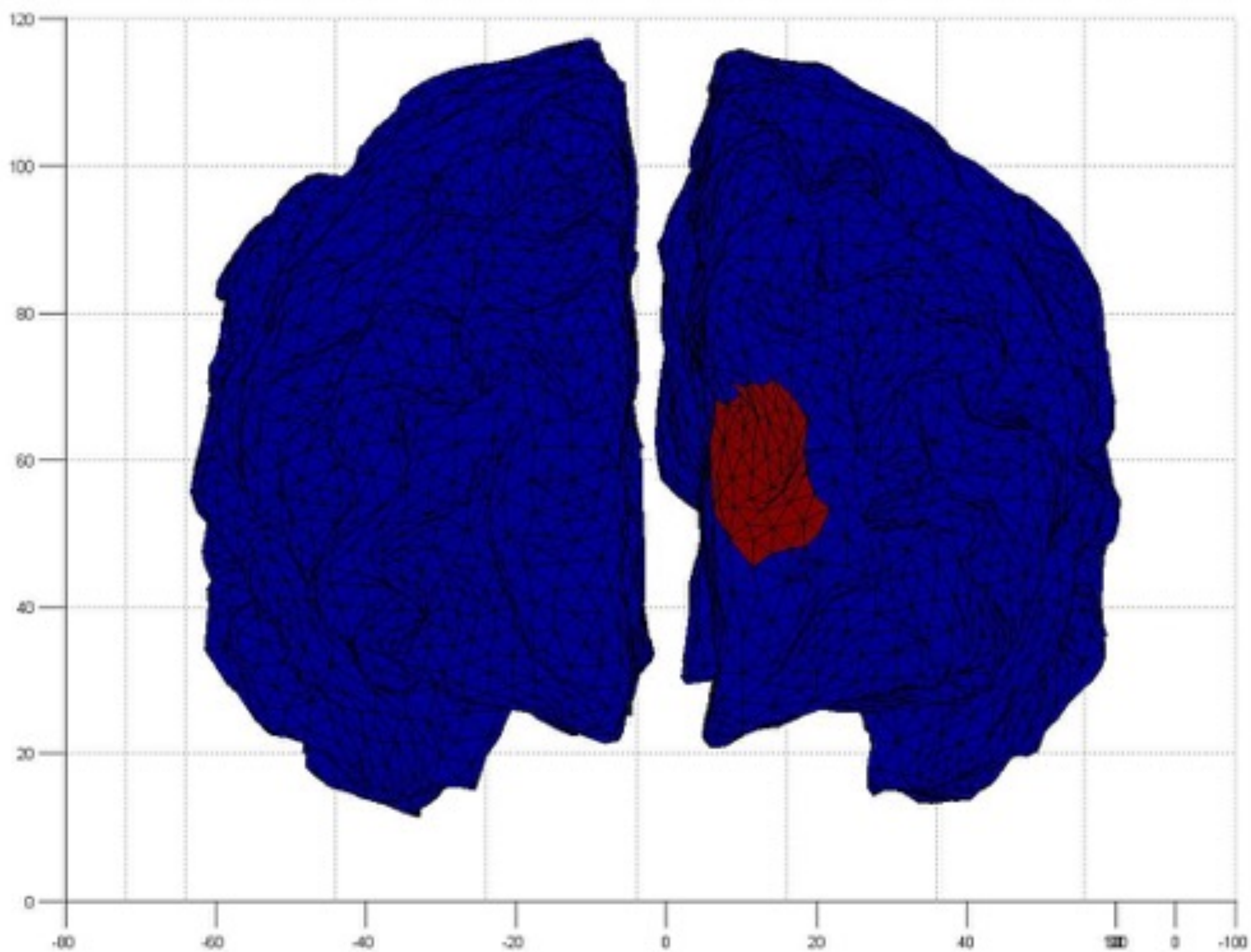

4.2 Distributed source localization results: Disk algorithm

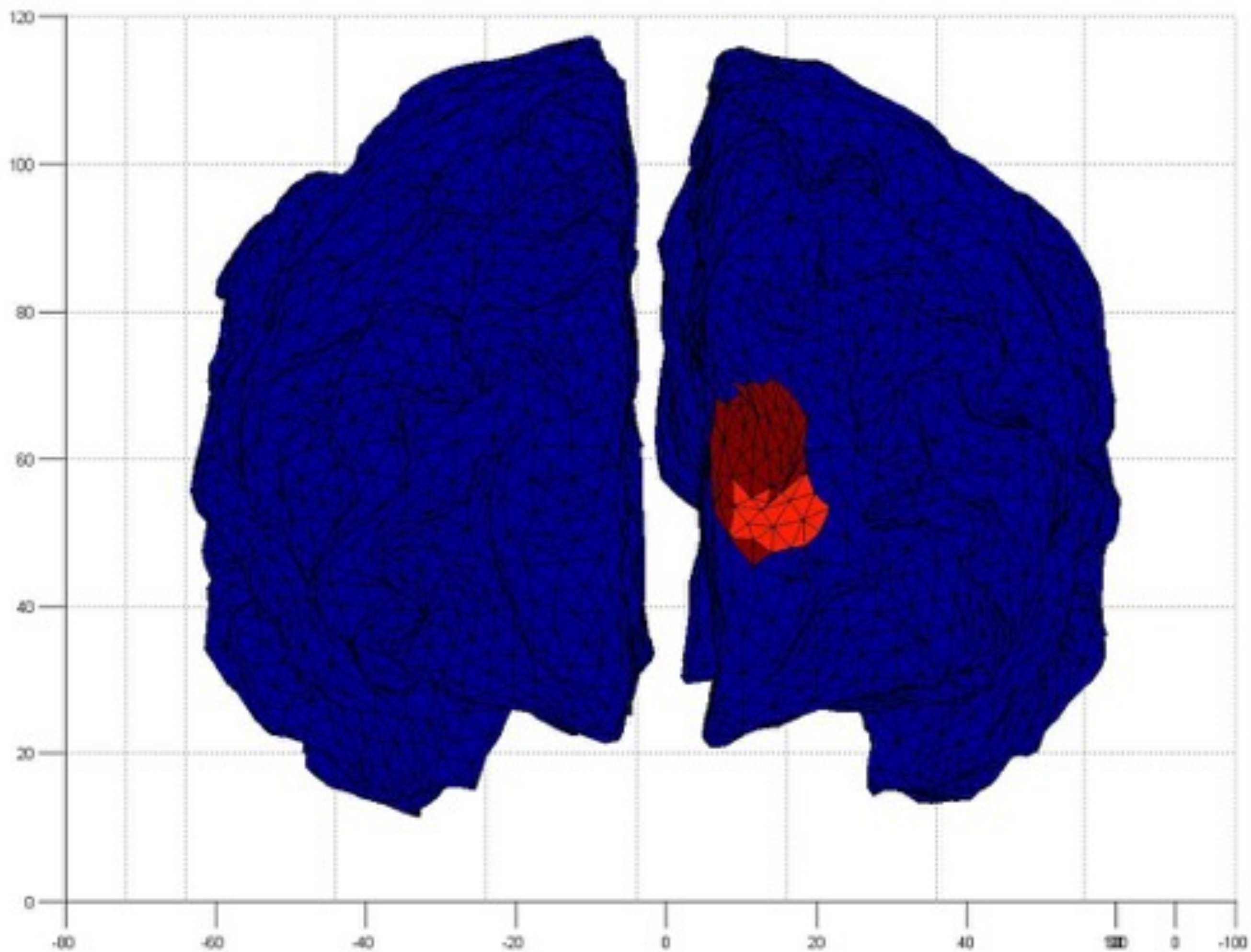

4.2 Distributed source localization results: Disk algorithm

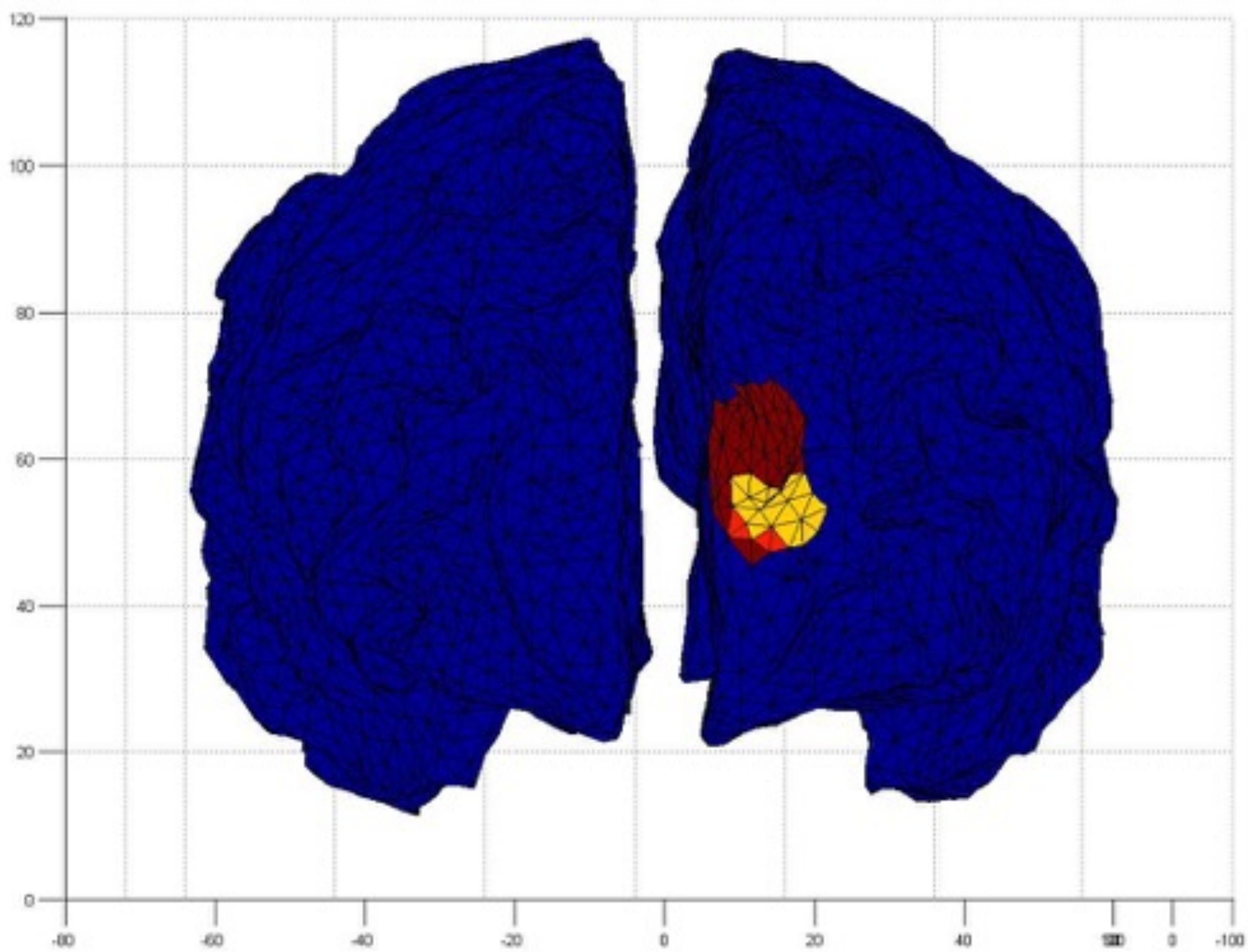

4.2 Distributed source localization results: Disk algorithm

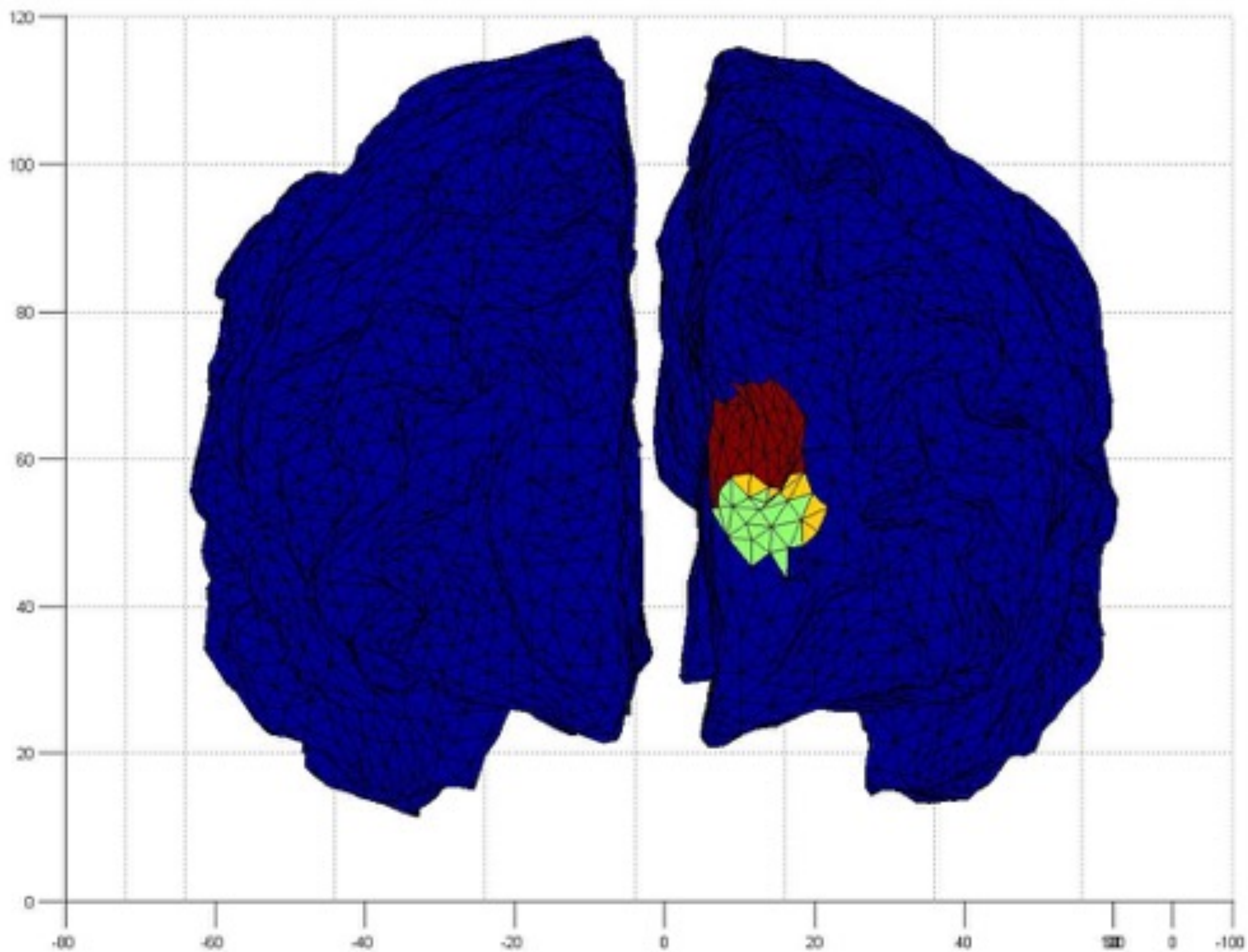

4.2 Distributed source localization results: Disk algorithm

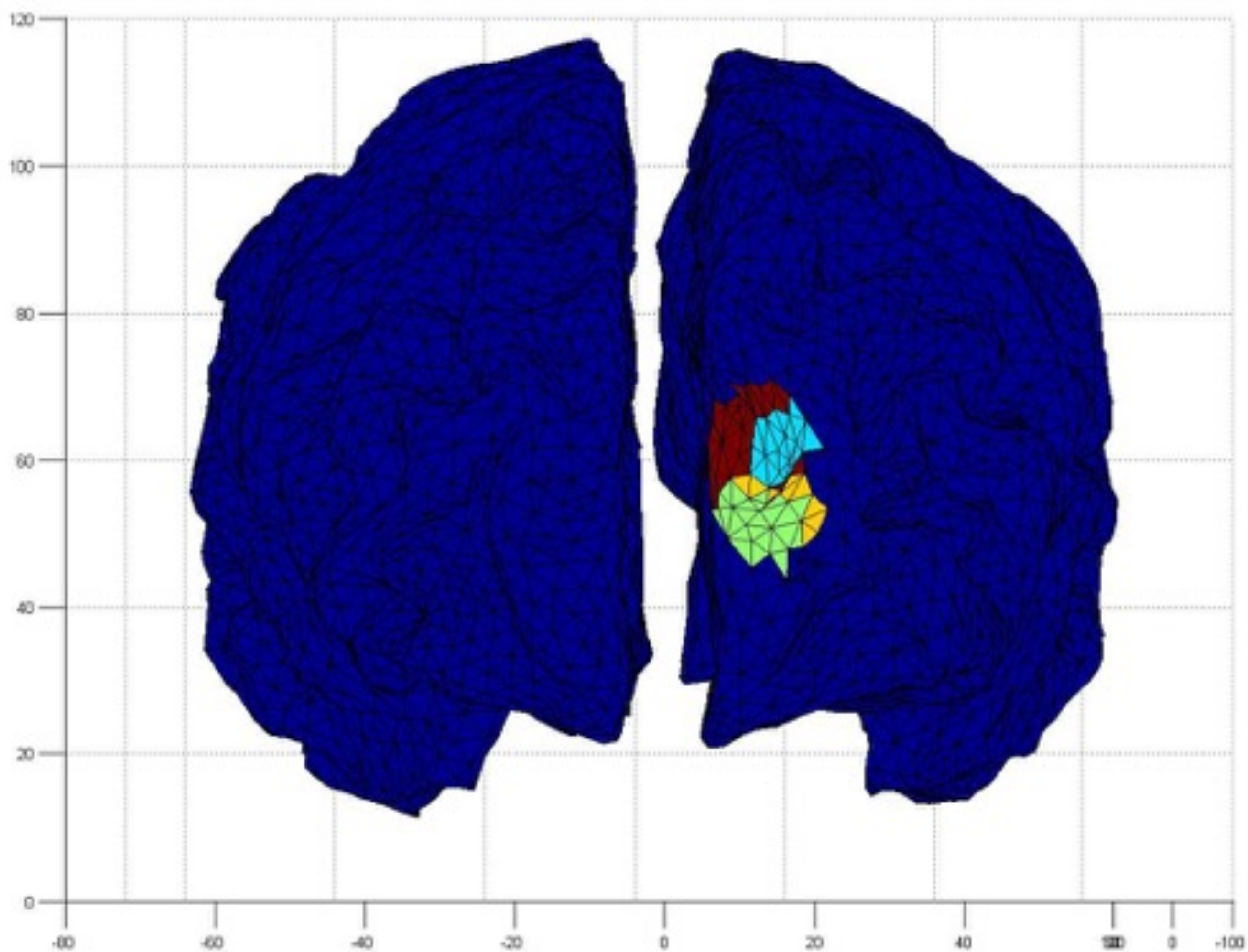

4.2 Distributed source localization results: Disk algorithm

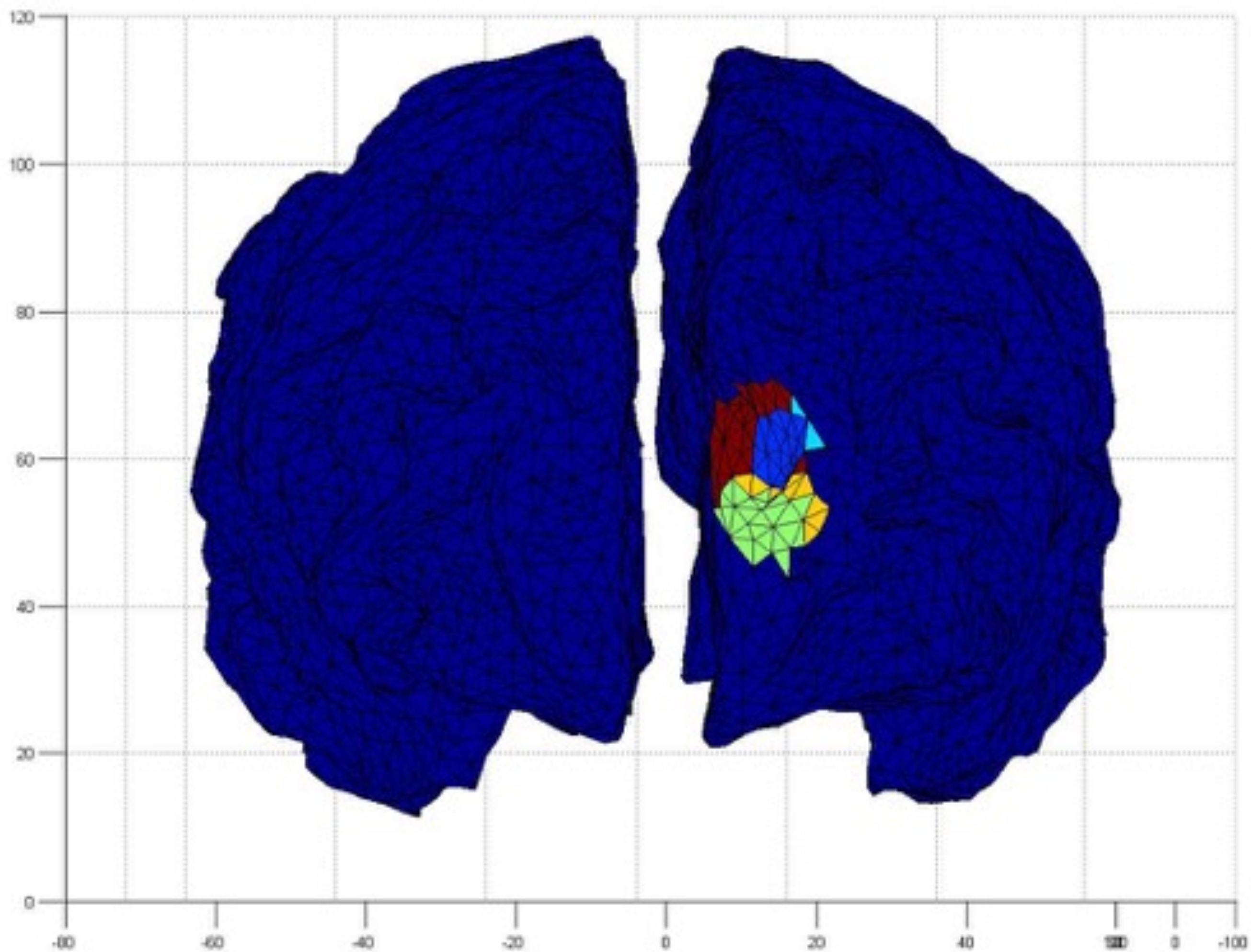

4.3 Proposed single-step approach: STS-SISSY (1)

- **Idea: Perform tensor decomposition and source localization in a single step**
  - **Impose structural constraint:** $\mathbf{H} = \mathbf{G}\mathbf{\Psi}$ **Piecewise-constant spatial distribution**
  - **Employ fused LASSO regularization:** $\lambda(||\mathbf{T}\mathbf{\Psi}||_1 + \alpha||\mathbf{\Psi}||_1)$

gradient operator

$\lambda,\ \alpha$ – regularization parameters

4.3 Proposed single-step approach: STS-SISSY (1)

- **Idea: Perform tensor decomposition and source localization in a single step**
  - **Impose structural constraint:** $\mathbf{H} = \mathbf{G}\boldsymbol{\Psi}$ **Piecewise-constant spatial distribution**
  - **Employ fused LASSO regularization:** $\lambda(||\mathbf{T}\boldsymbol{\Psi}||_1 + \alpha||\boldsymbol{\Psi}||_1)$

gradient operator

$\lambda,\ \alpha$ $-$ regularization parameters

- Constrained tensor decomposition based on ALS algorithm:

4.3 Proposed single-step approach: STS-SISSY (1)

- **Idea: Perform tensor decomposition and source localization in a single step**
  - **Impose structural constraint:** $\mathbf{H} = \mathbf{G}\boldsymbol{\Psi}$ **Piecewise-constant spatial distribution**
  - **Employ fused LASSO regularization:** $\lambda(||\mathbf{T}\boldsymbol{\Psi}||_1 + \alpha||\boldsymbol{\Psi}||_1)$

gradient operator

$\lambda,\ \alpha$ − regularization parameters

- Constrained tensor decomposition based on ALS algorithm:

$$\min_{\mathbf{H},\boldsymbol{\Psi}} ||\mathbf{X}^{(1)} - \mathbf{H}(\mathbf{C} \odot \mathbf{S})^{\mathrm{T}}||_{\mathrm{F}}^2 + \lambda(||\mathbf{T}\boldsymbol{\Psi}||_1 + \alpha||\boldsymbol{\Psi}||_1)$$

$$\text{s. t.} \quad \mathbf{H} = \mathbf{G}\boldsymbol{\Psi}$$

$\mathbf{X}^{(i)}$: unfolding $\mathbf{X}$ through its i-th direction

$$\min_{\mathbf{S}} ||\mathbf{X}^{(2)} - \mathbf{S}(\mathbf{C} \odot \mathbf{H})^{\mathrm{T}}||_{\mathrm{F}}^2$$

$$\min_{\mathbf{C}} ||\mathbf{X}^{(3)} - \mathbf{C}(\mathbf{S} \odot \mathbf{H})^{\mathrm{T}}||_{\mathrm{F}}^2$$

4.3 Proposed single-step approach: STS-SISSY (1)

- **Idea: Perform tensor decomposition and source localization in a single step**
  - **Impose structural constraint:** $\mathbf{H} = \mathbf{G}\boldsymbol{\Psi}$ **Piecewise-constant spatial distribution**
  - **Employ fused LASSO regularization:** $\lambda(||\mathbf{T}\boldsymbol{\Psi}||_1 + \alpha||\boldsymbol{\Psi}||_1)$

gradient operator

$\lambda,\ \alpha$ − regularization parameters

- Constrained tensor decomposition based on ALS algorithm:

$$\min_{\mathbf{H},\boldsymbol{\Psi}} ||\mathbf{X}^{(1)} - \mathbf{H}(\mathbf{C} \odot \mathbf{S})^{\mathrm{T}}||_{\mathrm{F}}^2 + \lambda(||\mathbf{T}\boldsymbol{\Psi}||_1 + \alpha||\boldsymbol{\Psi}||_1) \Longrightarrow ?$$

$$\text{s. t.} \quad \mathbf{H} = \mathbf{G}\boldsymbol{\Psi}$$

$\mathbf{X}^{(i)}$: unfolding $\mathbf{X}$ through its i-th direction

$$\min_{\mathbf{S}} ||\mathbf{X}^{(2)} - \mathbf{S}(\mathbf{C} \odot \mathbf{H})^{\mathrm{T}}||_{\mathrm{F}}^2 \Longrightarrow \mathbf{S} = \mathbf{X}^{(2)}\left((\mathbf{C} \odot \mathbf{H})^{\mathrm{T}}\right)^{+}$$

$$\min_{\mathbf{C}} ||\mathbf{X}^{(3)} - \mathbf{C}(\mathbf{S} \odot \mathbf{H})^{\mathrm{T}}||_{\mathrm{F}}^2 \Longrightarrow \mathbf{C} = \mathbf{X}^{(3)}\left((\mathbf{S} \odot \mathbf{H})^{\mathrm{T}}\right)^{+}$$

4.4 Proposed single-step approach: STS-SISSY (2)

- **Reformulation of the constrained optimization problem:**

$$\min_{\mathbf{H},\mathbf{Y},\mathbf{Z}} ||\mathbf{X}^{(1)} - \mathbf{H}(\mathbf{C}\odot\mathbf{S})^{\mathrm{T}}||_{\mathrm{F}}^2 + \lambda(||\mathbf{Y}||_1 + \alpha||\mathbf{Z}||_1)$$

$$\text{s. t.} \quad \mathbf{H} = \mathbf{G}\mathbf{\Psi},\ \mathbf{Y} = \mathbf{T}\mathbf{\Psi},\ \mathbf{Z} = \mathbf{\Psi}$$

- **Solution using ADMM with update equations:**

$$\mathbf{H} = (\mathbf{X}^{(1)}(\mathbf{C}\odot\mathbf{S}) + \rho\mathbf{G}\mathbf{\Psi} + \mathbf{V})((\mathbf{C}\odot\mathbf{S})^{\mathrm{T}}(\mathbf{C}\odot\mathbf{S}) + \rho\mathbf{I}_P)^{-1}$$

$$\mathbf{\Psi} = (\rho\mathbf{T}^{\mathrm{T}}\mathbf{T} + \rho\mathbf{I}_D + \rho\mathbf{G}^{\mathrm{T}}\mathbf{G})^{-1}\mathbf{\Phi}$$

with $\mathbf{\Phi} = \rho(\mathbf{T}^{\mathrm{T}}\mathbf{Y} + \mathbf{Z} + \mathbf{G}^{\mathrm{T}}(\mathbf{H} - \mathbf{V})) - \mathbf{T}^{\mathrm{T}}\mathbf{U} - \mathbf{W}$

  - **Latent variables:**

$$\mathbf{Y} = prox_{||\cdot||_1, \frac{\lambda}{\rho}}(\mathbf{T}\mathbf{\Psi} + \mathbf{U}/\rho)$$

$$\mathbf{Z} = prox_{||\cdot||_1, \frac{\lambda\alpha}{\rho}}(\mathbf{\Psi} + \mathbf{W}/\rho)$$

  - **Lagrangian multipliers:**

$$\Delta\mathbf{U} = \rho(\mathbf{T}\mathbf{\Psi} - \mathbf{Y});\ \Delta\mathbf{V} = \rho(\mathbf{G}\mathbf{\Psi} - \mathbf{H});\ \Delta\mathbf{W} = \rho(\mathbf{\Psi} - \mathbf{Z})$$

5. Simulation setup

- Realistic head model

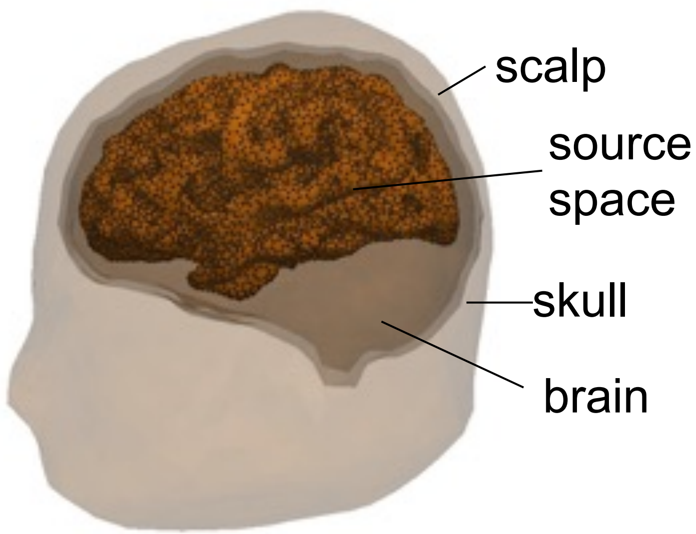

- SEEG signals for patch dipoles

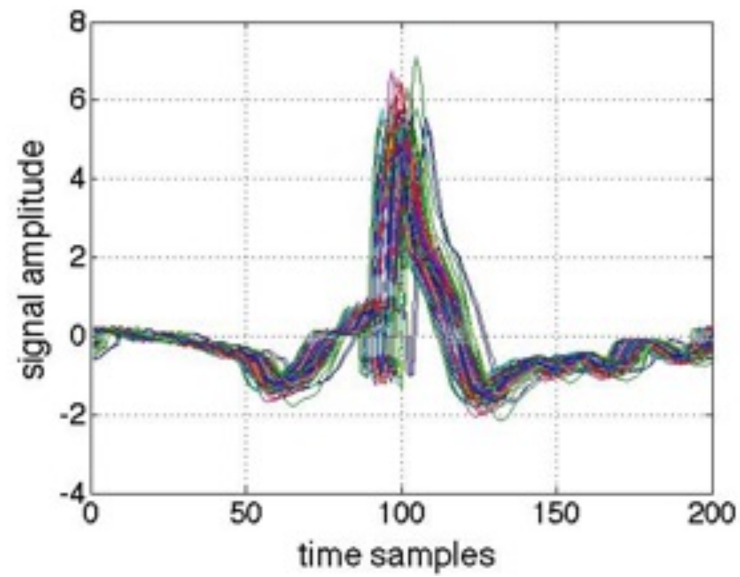

- Extended sources (patches) composed of adjacent grid dipoles
- Highly correlated interictal epileptic spike activities within a patch
- Two sources:
  - One source composed of two patches with delayed spike-like signals
  - One source composed of one patch with spike-like signals of slightly different morphology than for the first source
- 91 sensors, 50 realizations of spikes with different amplitudes

5.1 Evaluation criterion and performance results

- **Evaluation criterion: dipole localization error (DLE)**

$$\mathrm{DLE} = \frac{1}{2}\left(\frac{1}{\#\mathcal{I}}\sum_{k\in\mathcal{I}}\min_{\ell\in\hat{\mathcal{I}}}||\mathbf{r}_k - \mathbf{r}_\ell|| + \frac{1}{\#\hat{\mathcal{I}}}\sum_{\ell\in\hat{\mathcal{I}}}\min_{k\in\mathcal{I}}||\mathbf{r}_k - \mathbf{r}_\ell||\right)$$

$\mathcal{I}$ – Set containing the indices of active grid dipoles

$\hat{\mathcal{I}}$ – Set containing the indices of estimated active grid dipoles

$\mathbf{r}_k$ – Position of the k-th grid dipole

- **Performance results for two scenarios:**

scenario	Single-step STS-SISSY	Two-step STS-DA
1	1.32	18.23
2	1.37	7.29

Scenario 1

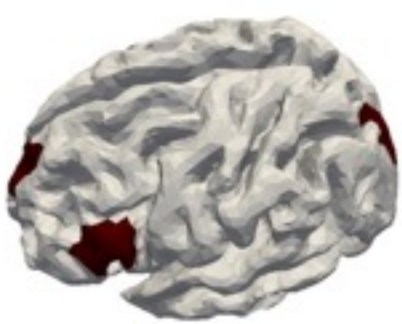

Scenario 2

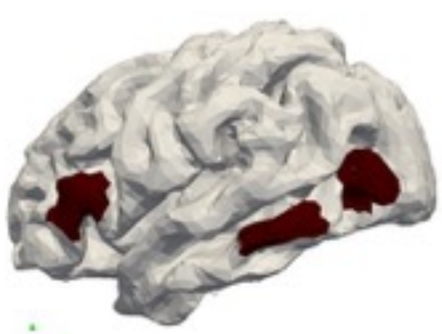

5.2 Illustration of simulation results

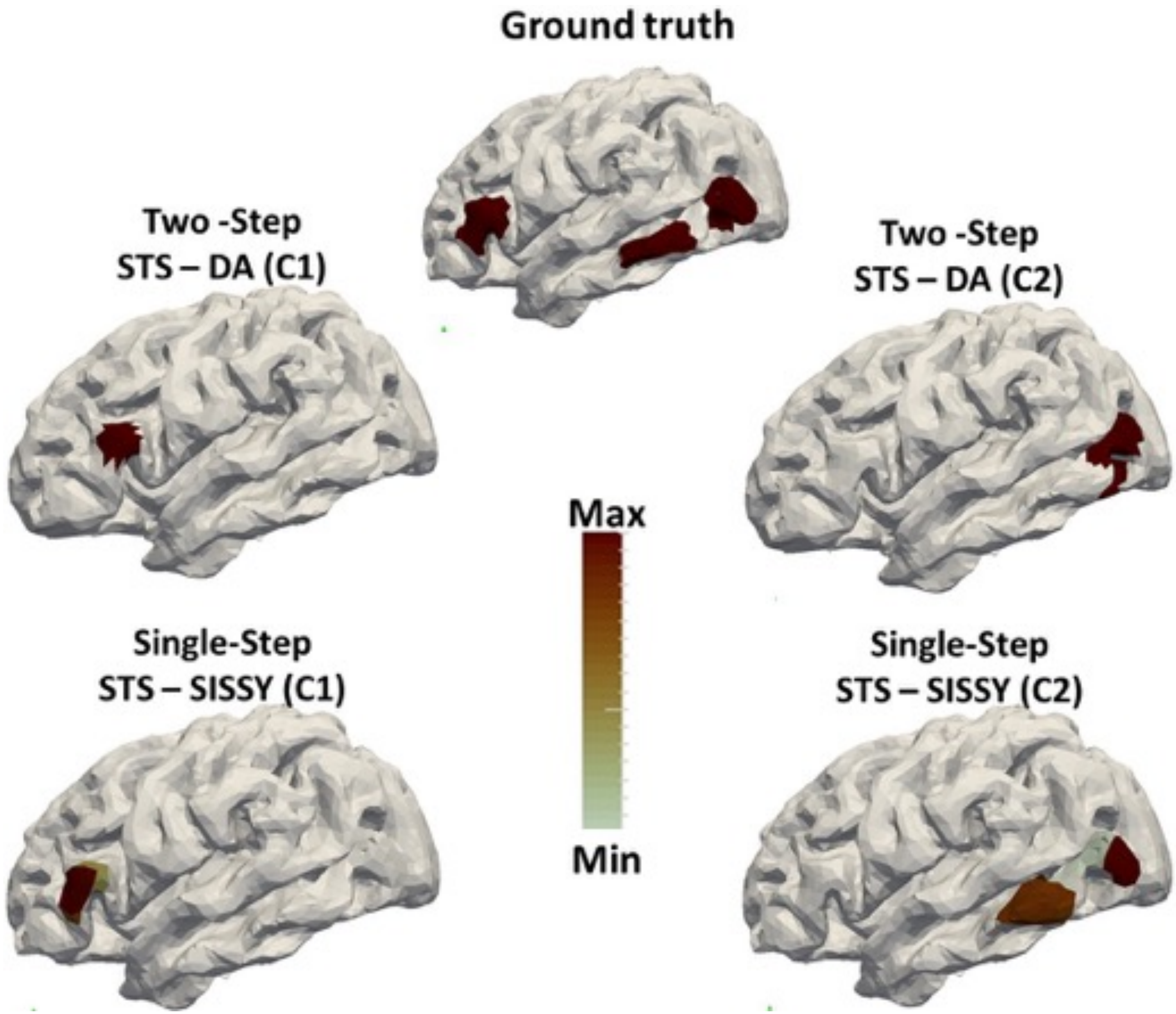

6. Conclusions

- EEG sources can be separated and localized in a single step by the proposed constrained tensor decomposition approach
- The proposed algorithm makes use of the ALS and ADMM optimization strategies
- Realistic simulations in the context of drug-resistant epilepsy have shown that the proposed single-step method outperforms a previously developed two-step tensor-based source localization approach

References (1)

[1] F. Miwakeichi, E. Martinez-Montes, P. A. Valdes-Sosa, N. Nishiyama, H. Mizuhara, and Y. Yamaguchi, "Decomposing EEG data into space-time-frequency components using parallel factor analysis," NeuroImage, 2004.

[2] H. Becker, P. Comon, L. Albera, M. Haardt, and I. Merlet, "Multi-way space-time-wave-vector analysis for EEG source separation," Signal Processing, 2012

[3] M. Morup, L. K. Hansen, C. S. Herrmann, J. Parnas, and S. M. Arnfred, "Parallel factor analysis as an exploratory tool for wavelet transformed event-related EEG," NeuroImage, 2006

[4] W. Deburchgraeve, P. J. Cherian, M. De Vos, R. M. Swarte, J. H. Blok, G. H. Visser, P. Govaert, and S. Van Huffel, "Neonatal seizure localization using Parafac decomposition," Clinical Neurophysiology, 2009

[5] M. Weis, D Jannek, T Guenther, P Husar, F. Roemer, M. Haardt, "Temporally resolved multi-way component analysis of dynamic sources in event-related EEG data using PARAFAC2," Proc. of EUSIPCO 2010

References (2)

[6] M. Morup, L. K. Hansen, S. M. Arnfred, L.-H. Lim, and K. H. Madsen, “Shift-invariant multilinear decomposition of neuroimaging data,” NeuroImage, 2008

[7] B. Hunyadi, D. Camps, L. Sorber, W. Van Paesschen, M. De Vos, S. Van Huffel, and L. De Lathauwer, “Block term decomposition for modelling epileptic seizures,” EURASIP Journal on Advances in Signal Processing, 2014

[8] H. Becker, L. Albera, P. Comon, M. Haardt, G. Birot, F. Wendling, M. Gavaret, C. G. B´enar, and I. Merlet, “EEG extended source localization: tensor-based vs. conventional methods,” NeuroImage, 2014